



ORIGINAL RESEARCH

Open Access



# Single-nucleus transcriptomic atlas of glial cells in human dorsal root ganglia

Donghang Zhang<sup>1,2†</sup>, Yiyong Wei<sup>3†</sup>, Yali Chen<sup>1,2</sup>, Hongjun Chen<sup>4</sup>, Jin Li<sup>5</sup>, Yaoxin Yang<sup>1,2</sup> and Cheng Zhou<sup>2\*</sup>

## Abstract

**Purpose** Glial cells play a crucial role in regulating physiological and pathological functions, such as sensation, infections, acute injuries, and chronic neurodegenerative disorders. Despite the recent understanding of glial subtypes and functional heterogeneity in central nervous system via single-cell/nucleus RNA sequencing, the transcriptomic profiles of glial cells in the adult human dorsal root ganglia (DRG) have not yet been characterized at single-cell resolution.

**Methods** We used high-throughput single-nucleus RNA sequencing to map the cellular and molecular heterogeneity of satellite glial cells (SGCs) and Schwann cells (SCs) in the human DRG, and further compared these human findings with those from mice. The expression profiles of classical marker genes of peripheral somatosensory system in glial cells were examined in human and mouse DRG. Additionally, the functional properties of the enriched genes in glial cells and their subtypes were also explored by Gene Ontology (GO) term analysis.

**Results** Human DRG cells were initially classified into 11 clusters based on their distinct transcriptional characteristics. SGCs and SCs were identified through their representative marker genes. SGCs were further classified into six subclusters, while SCs were classified into seven subclusters. The comparison with mouse transcriptomic profiles revealed an overall similarity between the two species, while simultaneously highlighting some degree of heterogeneity in specific genes.

**Conclusions** This atlas comprehensively profiled glial cell heterogeneity and provides a powerful resource for investigating the cellular basis of physiological and pathological conditions associated with DRG glial cells.

**Keywords** Dorsal root ganglia, Glial cells, Single nucleus RNA-sequencing

<sup>†</sup>Donghang Zhang and Yiyong Wei contributed equally to this work.

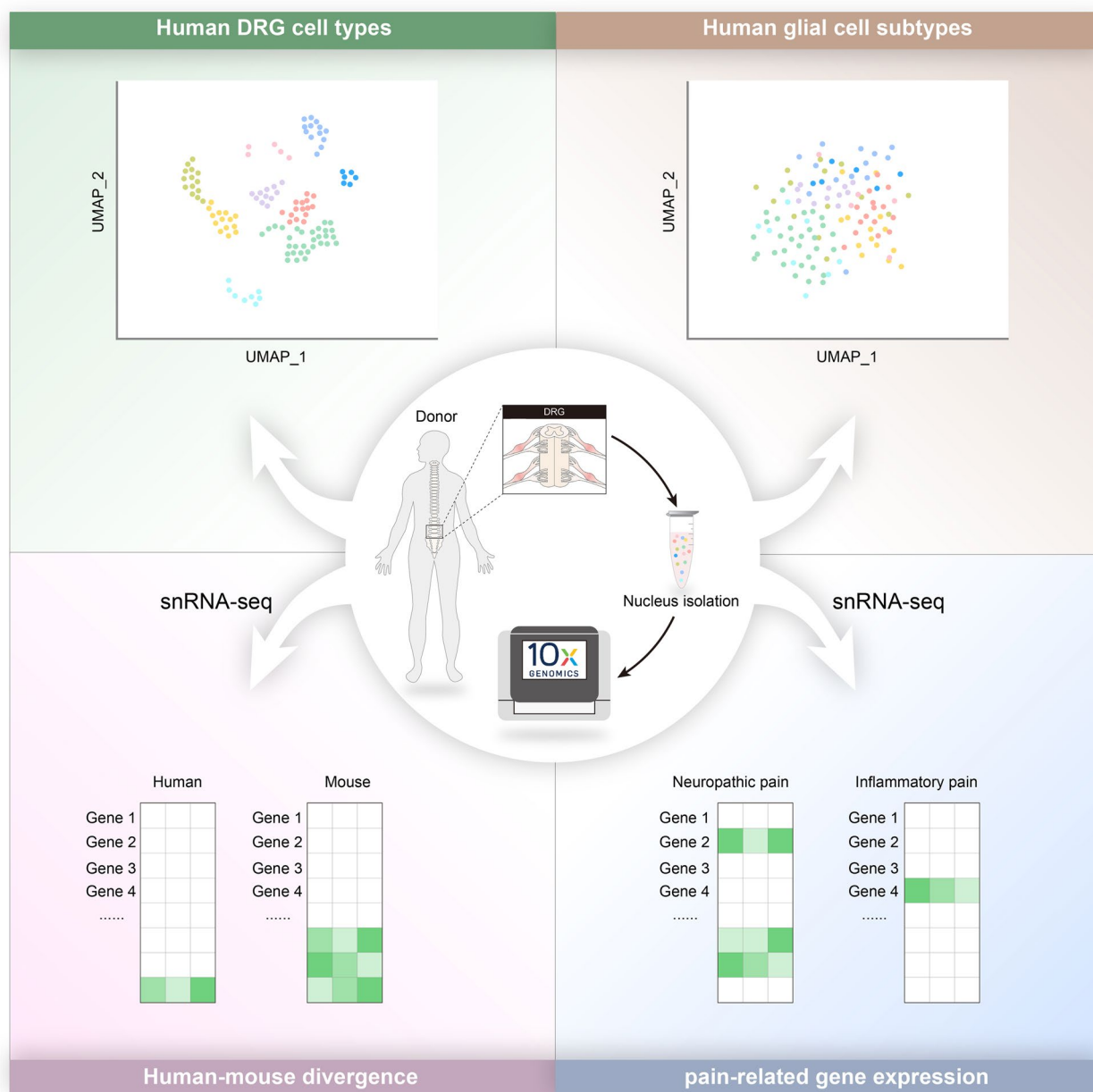
\*Correspondence:

Cheng Zhou  
zhouc@163.com

Full list of author information is available at the end of the article



**Graphical Abstract**



**1 Introduction**

Glial cells are abundantly present in both the peripheral (PNS) and central nervous system (CNS). The common types of glial cells in the CNS include astrocytes, microglia, and oligodendrocytes [1, 2]. In the PNS, satellite glial cells (SGCs) and Schwann cells (SCs) are the major glial types [3, 4]. In dorsal root ganglia (DRG), primary sensory neurons are wrapped by SGCs, and the interaction between

neurons and SGCs affect the nociceptive transmission [5]. Emerging evidence suggests that SGCs respond to pathological conditions within the peripheral nerves [6], and act as key modulators in chronic pain [7, 8]. Schwann cells (SCs) are another common type of glial cells in PNS. SCs are not only of fundamental physiological importance for myelin formation around peripheral axons, but also promote nerve regeneration after nerve injury [9].

Despite the clear evidence that glial cells play a pivotal role in sensory perception, processing as well as motor behavior, their cellular and functional heterogeneity are not well understood. Recently, emerging evidence has revealed cellular and molecular heterogeneity in glial cells of the CNS using single-cell (scRNA-seq) or single-nucleus RNA sequencing (snRNA-seq) [3, 5–11]. For example, using scRNA-seq, Hasel et al. identified 10 astrocyte subclusters in the mouse brain which showed heterogeneous responses to inflammation [8]. The knowledge about the cellular and functional heterogeneity of glial cells in PNS is significantly less than that in the CNS. Van Weperen et al. performed scRNA-seq on mouse stellate ganglia and divided SGCs into six distinct transcriptomic subtypes [3]. Yang et al. provided a cell atlas of human and mouse trigeminal ganglia at single-cell resolution, which identified neuronal and non-neuronal cell types, including SGCs and SCs that engaged in migraine and two mouse models of headache [12]. In human DRG, although recent studies have characterized the heterogeneity of neuronal subtypes using single-nucleus or spatial transcriptomic analysis [13, 14], to the best of our knowledge, no evidence of transcriptomic profiles of DRG glial cells at single-cell resolution is available.

In this study, we used 10×Genomics snRNA-seq to map the heterogeneity of glial cells, including SGCs and SCs, in the human DRG. Additionally, we addressed interspecies heterogeneity by comparing human and mouse transcriptomic profiles. This study aimed to serve as an important resource for future research on the molecular basis of human physiological and pathological conditions related to DRG glial cells.

## 2 Methods

### 2.1 Ethics approval

This study has been approved by the Ethical Committee of the Affiliated Hospital of Zunyi Medical University (Approval No. KLL-2020–273, May 19, 2021) and registered in the Chinese Clinical Trial Registry ([www.chictr.org.cn](http://www.chictr.org.cn)) on June 20, 2021 (ChiCTR2100047511). Written informed consent was signed before patient enrollment. The study protocol was in consistent with the ethical and legal guidelines.

### 2.2 Human samples

The lumbar L3–5 DRGs were acutely isolated from adult brain-dead human donors (two males, 38 and 46 years old; one female, 35 years old) within 90 min of cross-clamp in the operating room. These donors had not been diagnosed with acute/chronic low back or lower limb pain, two were dead from cerebral hernia and one was dead from intraventricular hemorrhage. Surgical procedures were performed by the same surgeon from department

of orthopedic surgery. Samples were immediately cleaned and frozen in liquid nitrogen for further use.

### 2.3 Isolation of nuclei

The nucleus was isolated using a Nucleus Isolation Kit (catalogue no. 52009–10, SHBIO, China) according to the manufacturer's protocols. Briefly, frozen human samples were thawed on ice, minced, and homogenized in cold 1% bovine serum albumin (BSA) in lysis buffer. The lysates were filtered through a 40- $\mu$ m cell strainer, followed by a centrifugation (500×g, 5 min) at 4 °C. Then, the pellets were resuspended in the lysis buffer after removing the supernatant. Phosphate buffered saline (PBS) were added and centrifuged (3000×g, 20 min) at 4 °C. The pellets were then filtered through a 40- $\mu$ m cell strainer, centrifuged (500 g, 5 min) at 4 °C, and resuspended twice in the nuclease-free BSA. Finally, nuclei were stained by trypan blue and counted using a dual-fluorescence cell counter.

### 2.4 cDNA synthesis

The nuclei suspension was loaded onto a Chromium single cell controller (10×Genomics) to produce single-nucleus gel beads in the emulsion (GEM) using single cell 3' Library and Gel Bead Kit V3.1 (10×Genomics, 1,000,075) and Chromium Single Cell B Chip Kit (10×Genomics, 1,000,074) according to the manufacturer's instructions. After the captured nucleus was lysed, the released mRNA was barcoded using reverse transcription in individual GEM. cDNA was generated by reverse transcription using a S1000TM Touch Thermal Cycler (Bio-Rad, 53 °C for 45 min, 85 °C for 5 min, and 4 °C until further use). The cDNA was then amplified and their quality was determined using an Agilent 4200 (CapitalBio Technology, Beijing).

### 2.5 10×Genomics library preparation and sequencing

The 10× snRNA-seq library was established using Single Cell 3' Library and Gel Bead Kit V3.1 according to the manufacturer's instructions. The library was sequenced using a Novaseq 6000 sequencing platform (Illumina) with a depth of at least 30,000 reads per nucleus with a paired-end 150 bp (PE150) reading strategy (CapitalBio Technology, Beijing).

### 2.6 Single-nucleus transcriptomic data analysis

#### 2.6.1 Data pre-processing

We first processed 10×Genomics raw data by the Cell Ranger Single-Cell Software Suite (release 5.0.1), including using cellranger mkfastq to demultiplex raw base call files into FASTQ files and then using cellranger count to perform alignment, filtering, barcode counting, and unique molecular identifier (UMI) counting. The reads

(including intron sequences) were aligned to the hg19 reference genome using a pre-built annotation package download from the 10× Genomics website.

### 2.6.2 Quality control

We performed quality control to remove low-quality cells, empty droplets or cell doublets. Low-quality cells or empty droplets often contain very few genes or exhibit extensive mitochondrial contamination, whereas cell doublets may exhibit an aberrantly high gene count. Moreover, we can detect contamination with low complexity cells like red blood cells that show a less complex RNA species. Specifically, cells were filtered out if the gene number was less than 200 or more than 8,000, UMI counts was less than 500, cell complexity was less than 0.8, or if the mitochondrial gene ratio was more than 10%.

### 2.6.3 Normalization and integration

Seurat package (4.1.0) was used to normalize and scale the single-nucleus gene expression data. Data was first normalized by “Normalize Data” function with setting normalization method as ‘Log Normalize’. In detail, the expression of gene A in cell B was determined by the UMI count of gene A divided by the total number of UMI of the cell B, followed by multiplying 10,000 for the normalization and the log-transformed counts were then computed with base as 2. Top 2,000 highly variable genes (HVGs) were detected by “Find Variable Features” function with setting selection method as “vst”. We then removed the uninteresting sources of variation by regressing out cell-cell variation within gene expression driven by batch, the number of detected UMI, mitochondrial gene expression, and ribosomal gene expression, which was implemented by “Scale Data” function. Finally, the corrected expression matrix was used as an input for further analysis.

### 2.6.4 Dimension reduction, cell clustering and annotation

“Run PCA” function in the Seurat package was used to perform the principal component analysis (PCA) on the single-cell expression matrix with genes restricted to HVGs. To integrate cells into a shared space from different batches for unsupervised clustering, harmony algorithm was used to integrate two batches, which was implemented by “Run Harmony” function. “Find Clusters” function in the Seurat package was then used to conduct the cell clustering analysis through embedding cells into a graph structure in harmony space. The clustering results were visualized using Uniform Manifold Approximation and Projection (UMAP). Multiple cell type-specific/enriched marker genes that have been previously described in the literature were used to determine cell-type identity, including *FABP7* and *APOE* for SGCs; and *MPZ*, *PMP22*, *PRX*, and *PLLP* for Schwann cells.

### 2.6.5 Differential expression analysis

Differential gene expression analysis was performed using the ‘Find Markers’ function, which performs differential expression based on the non-parametric Wilcoxon rank sum test for two annotated cell groups. The marker genes were identified using the ‘Find All Markers’ function in Seurat with settings on genes with at least 0.25 increasing logFC upregulation, comparing to the remaining cell clusters.

### 2.6.6 Enrichment analysis

Gene Ontology (GO) enrichment was conducted using R package with default settings. GO terms with an adjusted *p*-value of less than 0.05 that calculated by the hypergeometric test followed by the Benjamini–Hochberg method were defined as significantly enriched terms. The top 20 enriched terms were visualized.

### 2.6.7 Risk genes of diseases

The risk genes of diseases were identified using DisGeNET (<https://www.disgenet.org>), which contains one of the largest publicly available collections of genes associated with human diseases. The current version of DisGeNET (v7.0) contains 1,134,942 gene-disease associations (GDAs), between 21,671 genes and 30,170 diseases, disorders, traits, and clinical or abnormal human phenotypes. From the summary of GDAs, the top 50 risk genes ordered by the number of PMIDs were selected.

### 2.6.8 Comparison to RNA-seq data sets from mouse

For analysis of the mouse, the snRNA-seq data of naive DRGs from 8–12-week-old C57BL/6 J mice (strain #000,664; RRID: IMSR\_JAX: 000,664) was extracted from data deposited by Renthal et al. [15].

## 3 Results

### 3.1 Identification of glial cell types in human and mouse DRG

snRNA-seq was performed on 26,279 nuclei from the L3-L5 DRG of three adult donors (Fig. 1A). DRG cells were initially classified into 11 clusters based on their distinct transcriptional characteristics (Fig. 1B). We verified that each individual donor contributed nuclei to each cluster and the gene expression profiles correlated well among three donors (Supplementary Fig. 1). Transcriptomic analysis of DRG neurons (Cluster 10 in Fig. 1B, labeled with the representative markers *SNAP25* [*synaptosome associated protein 25*], *SYP* [*synaptophysin*], and *RBFOX3* [*RNA binding fox-1 homolog 3*]) were not performed due to the limited numbers captured by the nuclei-isolation method. Therefore, our present study focused on the transcriptomic data from glial cells. As a result, SGCs (10.7% of total nuclei) were

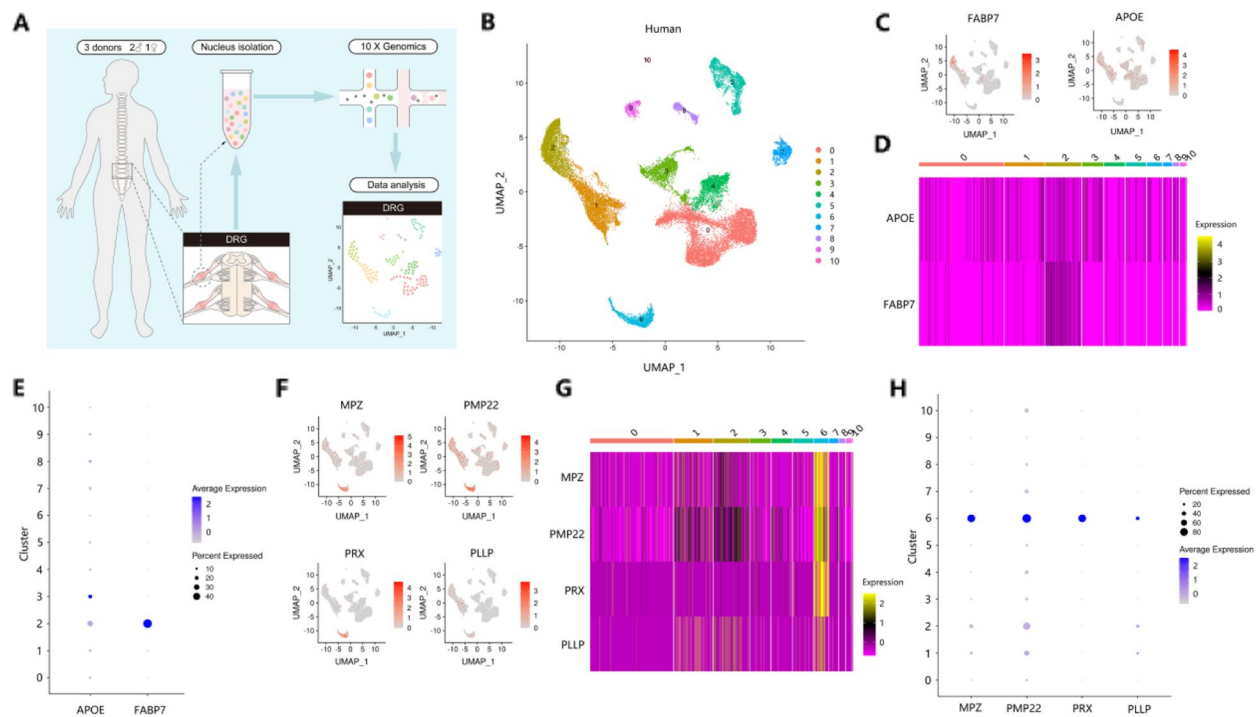


**Fig. 1** Identification of glial cell-types in human DRG. **A** Overview of the experimental workflow for snRNA-seq in DRG. **B** UMAP plot of human DRG cells showing 11 major cell types. Dots, individual cells; Colors, cell types. **C** UMAP plot showing the expression of representative well-known marker genes of human SGCs. Numbers reflect the number of UMIs detected for the specified gene in each cell. **D** Heatmap showing the distribution of expression levels of marker genes of human DRG SGCs across all 11 cell types. **E** Dot plot showing the distribution of expression levels of human SGCs marker genes across all cell types. **F** UMAP plot showing the expression of representative well-known marker genes of human SCs. **G** Heatmap showing the distribution of expression levels of marker genes of human DRG SCs across all cell types. **H** Dot plot showing the distribution of expression levels of human SCs marker genes across all cell types. DRG, dorsal root ganglia; UMAP, Uniform Manifold Approximation and Projection; SGCs, satellite glial cells; UMIs, unique molecular identifiers; SCs, Schwann cells

labeled with the representative markers *FABP7* (*fatty acid binding protein 7*) and *APOE* (*apolipoprotein E*) and formed Cluster 2 (Fig. 1C–E), and Schwann cells (5.8% of total nuclei) were identified with the representative markers *MPZ* (*myelin protein zero*), *PMP22* (*peripheral myelin protein 22*), *PRX* (*periaxin*), and *PLLP* (*plasmalipin*) as Cluster 6 (Fig. 1F–H). We also reanalyzed available snRNA-seq transcriptional data of the mouse DRG from a previous study [15]. DRG cells from seven C57 mice were classified into 22 cell types (Fig. 2A), of which Cluster 0 was identified as SGCs (9.8% of total nuclei) with the markers *Fabp7* and *Apoe* (Fig. 2B–D). Schwann cells (6% of total nuclei) were identified with the representative markers *Mpz*, *Pmp22*, *Prx*, and *Plp* as Cluster 6 (Fig. 2E–G). These findings suggest the fraction of glial subtypes in DRG was similar between humans and mice.

### 3.2 Identification of glial cell subtypes

To determine the heterogeneity within each glial cell type, SGCs were further classified into six subclusters in humans (Fig. 3A, B, Supplementary Fig. 2A) and

three subclusters in mice (Fig. 3C, D, Supplementary Fig. 2B). SCs were further classified into seven subclusters in humans (Fig. 4A, B, Supplementary Fig. 3A) and three subclusters in mice (Fig. 4C, D, Supplementary Fig. 3B). Regarding intraspecies comparison, SGCs and SCs showed substantial similarity across subtypes, as they could not be classified completely. While we also identified genes that are differentially expressed across subclusters, such as *CNTNAP2* (*encoding contactin associated protein 2, which mediates interactions between neurons and glia during nervous system development and is also involved in localization of potassium channels within differentiating axons*) (Fig. 3B), and *Neat1* (*encoding nuclear paraspeckle assembly transcript 1, which acts as a transcriptional regulator for numerous genes*) (Fig. 3D).

We further analyzed the representative marker genes which exhibited uniquely high expression levels in each subcluster, and finally identified several genes that associated with pain, such as *Prx* (*periaxin*) [16], *Stat1* (*signal transducer and activator of transcription 1*) [17] and *Cntf* (*ciliary neurotrophic factor*) [18] in mouse SCs



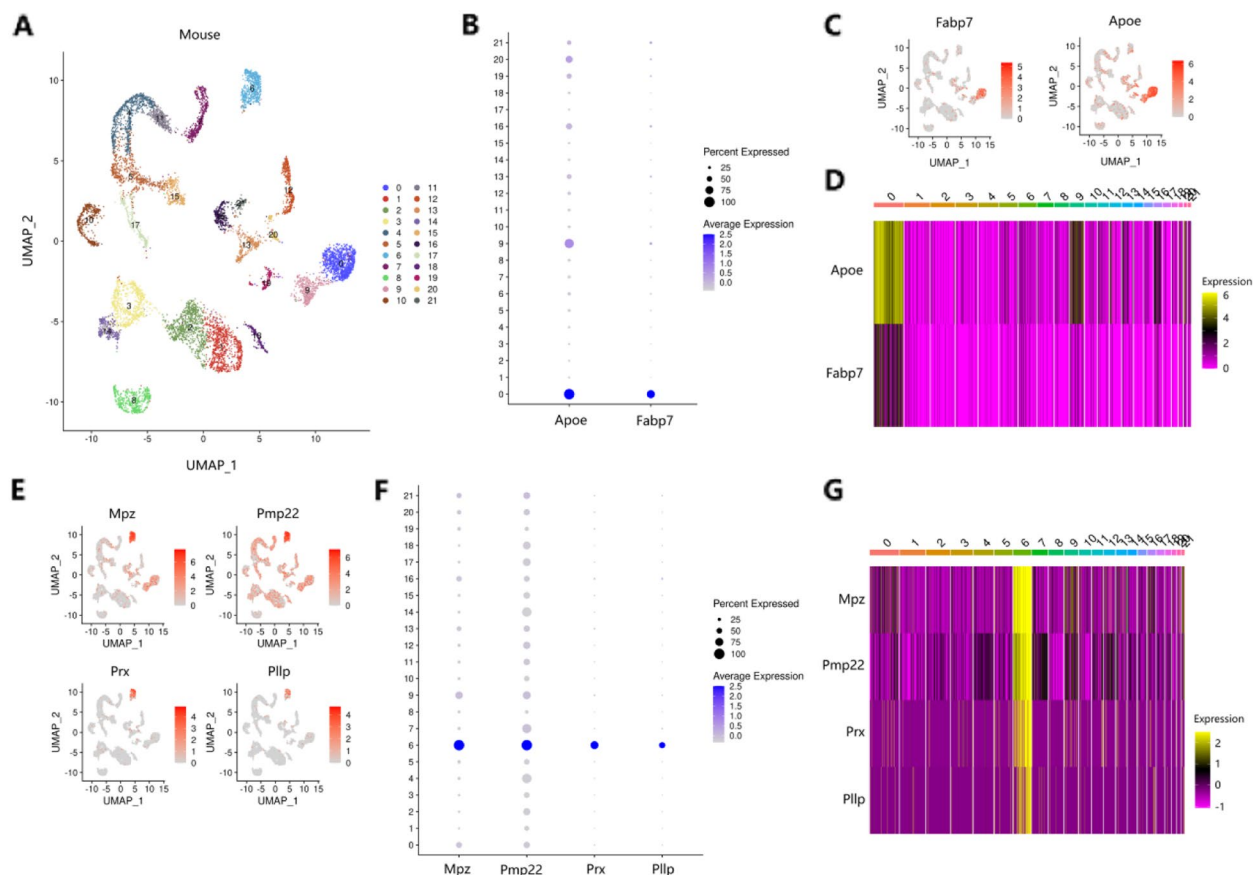


**Fig. 2** Identification of glial cell-types in mouse DRG. **A** UMAP plot of mouse DRG cells showing 22 major cell types. Dots, individual cells; Colors, cell types. **B** Dot plot showing the distribution of expression levels of mouse SGCs marker genes across all cell types. **C** UMAP plot showing the expression of representative well-known marker genes of mouse SGCs. **D** Heatmap showing the distribution of expression levels of marker genes of mouse DRG SGCs across all cell types. **E** UMAP plot showing the expression of representative well-known marker genes of mouse SCs. **F** Dot plot showing the distribution of expression levels of mouse SCs marker genes across all cell types. **G** Heatmap showing the distribution of expression levels of marker genes of mouse DRG SCs across all cell types. DRG, dorsal root ganglia; UMAP, Uniform Manifold Approximation and Projection; SGCs, satellite glial cells; SCs, Schwann cells

(Fig. 4D). Previous evidence also reported that several differentially expressed genes identified in our study was present in DRG and were involved in pain disorders, such as *FGF13* (fibroblast growth factor 13) [19], *PTGDS* (prostaglandin D2 synthase) [20] and *CNTNAP2* [21]; however, whether their function in glial cells was associated with pain requires to be determined. Interestingly, one study reported that neuropathic pain-associated *Pi16* (peptidase inhibitor 16) was not expressed in glia of mouse DRG [22], while our data showed that *PII6* was predominantly expressed in Cluster 4 of human SGCs.

### 3.3 Human-mouse divergence

To address the similarities and differences in glial cells between humans and mice, we performed co-clustering methods [23] to align human transcriptomic data with those from mice. Unlike DRG neuronal data that

clustered well between human and mouse as described in previous studies [14], alignment results of glial data suggested significant heterogeneity in SGCs (Supplementary Fig. 4A) or SCs (Supplementary Fig. 4B) between mice and humans, as indicated by the slight overlap across species.

Transcriptional profiles of classical markers of somatosensory system in glial cells between humans and mice were examined, including ion channels, neurotransmitter receptors, neuropeptides, and transcription factors (Figs. 5 and 6). Firstly, from this atlas, we can observe the differential expression patterns in the same family. For example, in the family of voltage-gated sodium channels, *SCN7A* (encoding *Nav2.1*) showed significantly higher expression than other subtypes did in human SGCs (Fig. 5A, left panel). For neurotransmitter receptors, *Grina* (encoding glutamate ionotropic receptor NMDA type subunit associated protein 1) exhibited extremely

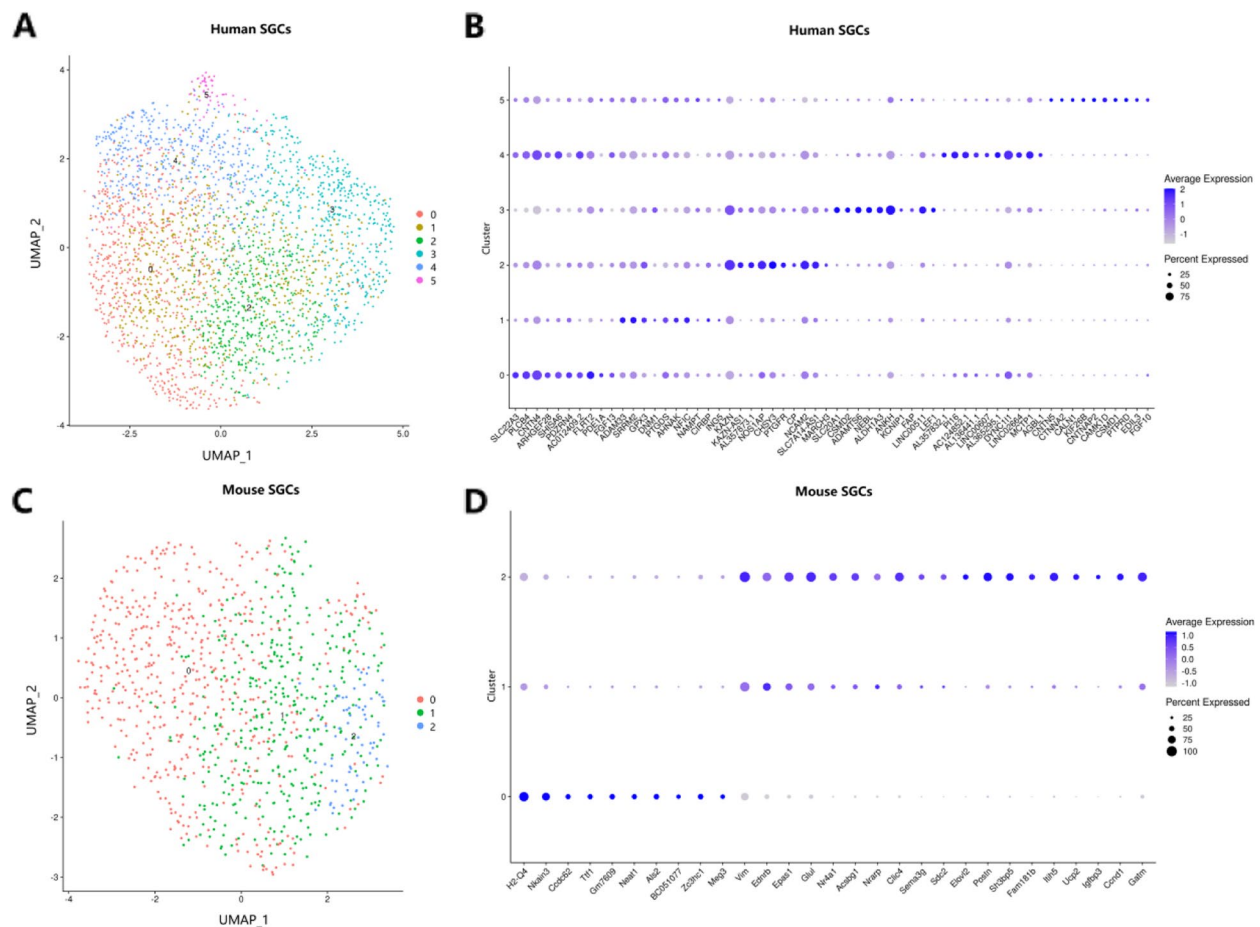


**Fig. 3** Identification of subtypes of DRG SGCs. **A** UMAP plot showing 6 clusters in human SGCs. Dots, individual cells; Colors, clusters. **B** Dot plot showing the expression of the top ten most differentially expressed genes across all the SGCs clusters in humans. **C** UMAP plot showing 3 clusters in mouse SGCs. Dots, individual cells; Colors, clusters. **D** Dot plot showing the expression of the top ten most differentially expressed genes across all the SGCs clusters in mice. DRG, dorsal root ganglia; UMAP, Uniform Manifold Approximation and Projection; SGCs, satellite glial cells

higher levels than other family members did in mouse SGCs (Fig. 5D, right panel). *SLC12A2* (encoding *NKCC1*) showed higher levels than *SLC12A5* (encoding *KCC2*) in both human and mouse SGCs (Fig. 5E). In the family of voltage-gated calcium channels, *CACNA1A* (encoding *Cav2.1*) showed significantly higher expression than other subtypes did in human and mouse SCs (Fig. 6B). Secondly, we compared the gene expression across different subclusters in humans and/or mice. Although most genes showed consistent patterns, a number of genes were significantly differentially expressed across subclusters. For examples, *HTR4* (encoding *5-hydroxytryptamine receptor 4*, which modulates the release of various neurotransmitters in both PNS and CNS) showed significantly higher expression levels in Cluster 5 than in other clusters in human DRG SGCs (Fig. 5E, left panel). *Adra1a* (encoding *Adrenoceptor alpha 1A*, which regulates cell growth and proliferation) showed significantly higher expression levels in Cluster 0 than in other clusters in

mouse DRG SGCs (Fig. 5E, right panel). *SCN7A* showed significantly higher levels in Cluster 6 than in other clusters in human DRG SCs (Fig. 6A, left panel). *GABRG3* (encoding *gamma-aminobutyric acid type A receptor subunit gamma3*) showed significantly higher expression levels in Cluster 5 than in other clusters in human DRG SCs (Fig. 6D, left panel).

Next, we compared the transcriptomic data of glial cells between humans and mice. While gene expression patterns between human and mouse DRG exhibit a high degree of similarity, we also identified genes that are differentially expressed between these two species. For examples, *CACNA1C* (encoding *calcium voltage-gated channel subunit alpha1 C that mediates inward  $Ca^{2+}$  influx upon membrane polarization*) expression was significantly higher than *CACNA1A* in human SGCs (Fig. 5B, left panel), but *Cacna1c* expression was lower than *Cacna1a* in mouse SGCs (Fig. 5B, right panel). *KCNK2* (encoding *TREK1 that leaks potassium out of the cell to control*

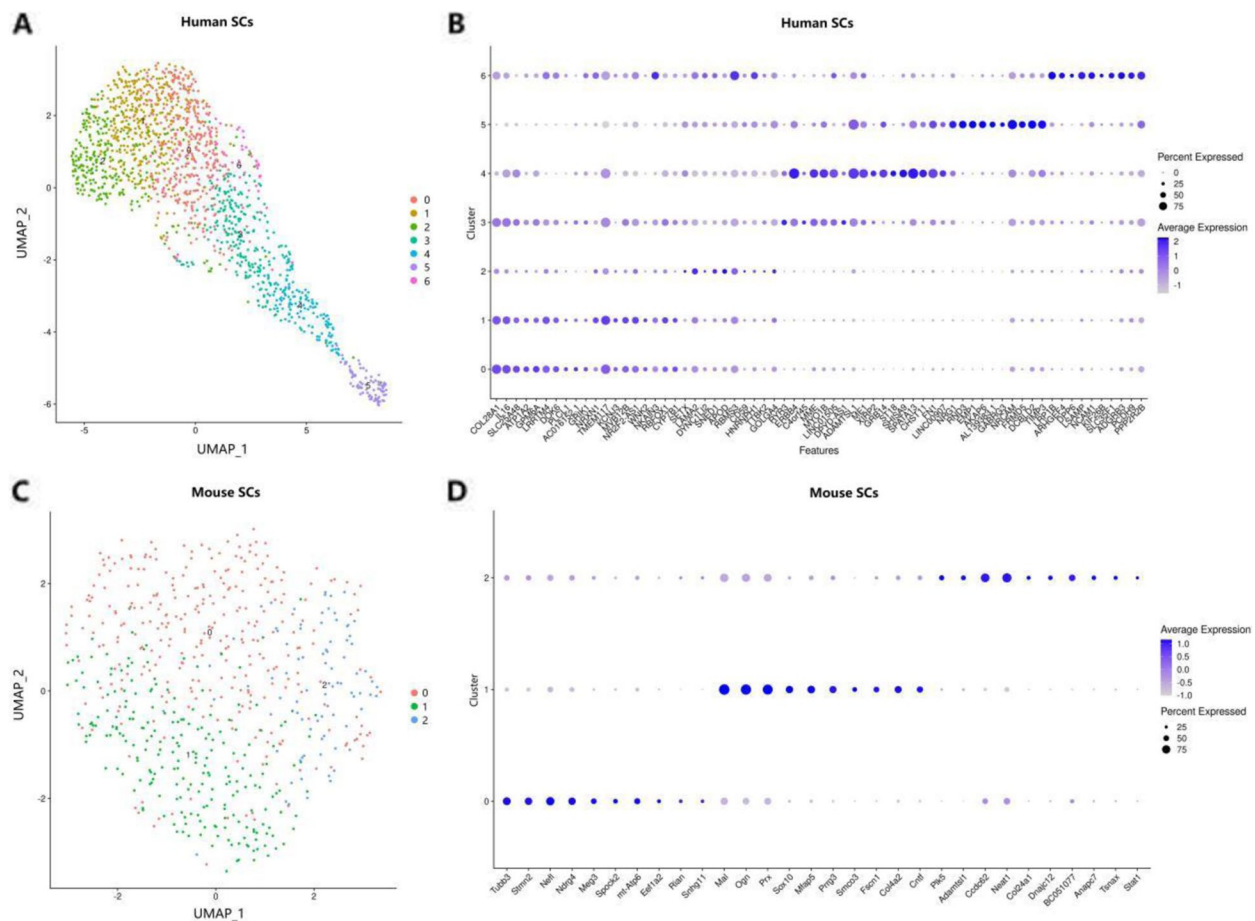


**Fig. 4** Identification of subtypes of DRG SCs. **A** UMAP plot showing 7 clusters in human SCs. Dots, individual cells; Colors, clusters. **B** Dot plot showing the expression of the top ten most differentially expressed genes across all the SCs clusters in humans. **C** UMAP plot showing 3 clusters in mouse SCs. Dots, individual cells; Colors, clusters. **D** Dot plot showing the expression of the top ten most differentially expressed genes across all the SCs clusters in mice. DRG, dorsal root ganglia; UMAP, Uniform Manifold Approximation and Projection; SCs, Schwann cells

resting membrane potential) expression was significantly higher than *KCNJ10* (encoding *KIR4.1*, which is responsible for the potassium buffering action of glial cells) in human SGCs (Fig. 5C, left panel), but *Kcnk2* expression was lower than *Kcnj10* in mouse SGCs (Fig. 5C, right panel). *RORA* (encoding *RAR* related orphan receptor A, which belongs to nuclear hormone receptors) expression was significantly higher than *MAF* (encoding *MAF* bZIP transcription factor, which acts as a transcriptional activator or repressor) in human SGCs (Fig. 5G, left panel), but *Rora* expression was lower than *Maf* in mouse SGCs (Fig. 5G, right panel). *PAM* (encoding *peptidylglycine alpha-amidating monooxygenase*, which catalyzes the conversion of neuroendocrine peptides to active alpha-amidated products) expression was significantly higher than *CALCA* (encoding *calcitonin gene-related peptide CGRP*, which functions as a vasodilator) in human SGCs (Fig. 5H, left panel), but *Pam* expression was lower than *Calca* in mouse SGCs (Fig. 5H, right panel). *KCNJ3* (encoding *Kir3.1*, which allows potassium

to flow into the cell) and *KCNK12* (encoding *Thik2*, which belongs to the superfamily of potassium channels containing two pore-forming P domains) expression was significantly higher than *KCNA1* (encoding *K<sub>V</sub>1.1*, which is associated with myokymia with periodic ataxia) and *KCNA2* (encoding *K<sub>V</sub>1.2*, which allows nerve cells to repolarize after action potentials) in human SCs (Fig. 6C, left panel), but *Kcna1* and *Kcna2* expression was lower than *Kcnj3* and *Kcnk12* in mouse SCs (Fig. 6C, right panel). *HCN1* (encoding *hyperpolarization activated cyclic nucleotide gated potassium channel 1*, which contributes to the native pacemaker currents in neurons.) expression was significantly higher than *SLC12A2* in human SCs (Fig. 6E, left panel), but *Hcn1* expression was lower than *Slc12a2* in mouse SCs (Fig. 6E, right panel). And *TACR1* (encoding *tachykinin receptor 1* for tachykinin substance P) expression was higher than *ADRA2A* (encoding *adrenoceptor alpha 2A*, which is required for presynaptic transmitter release from central noradrenergic neurons) in human SCs



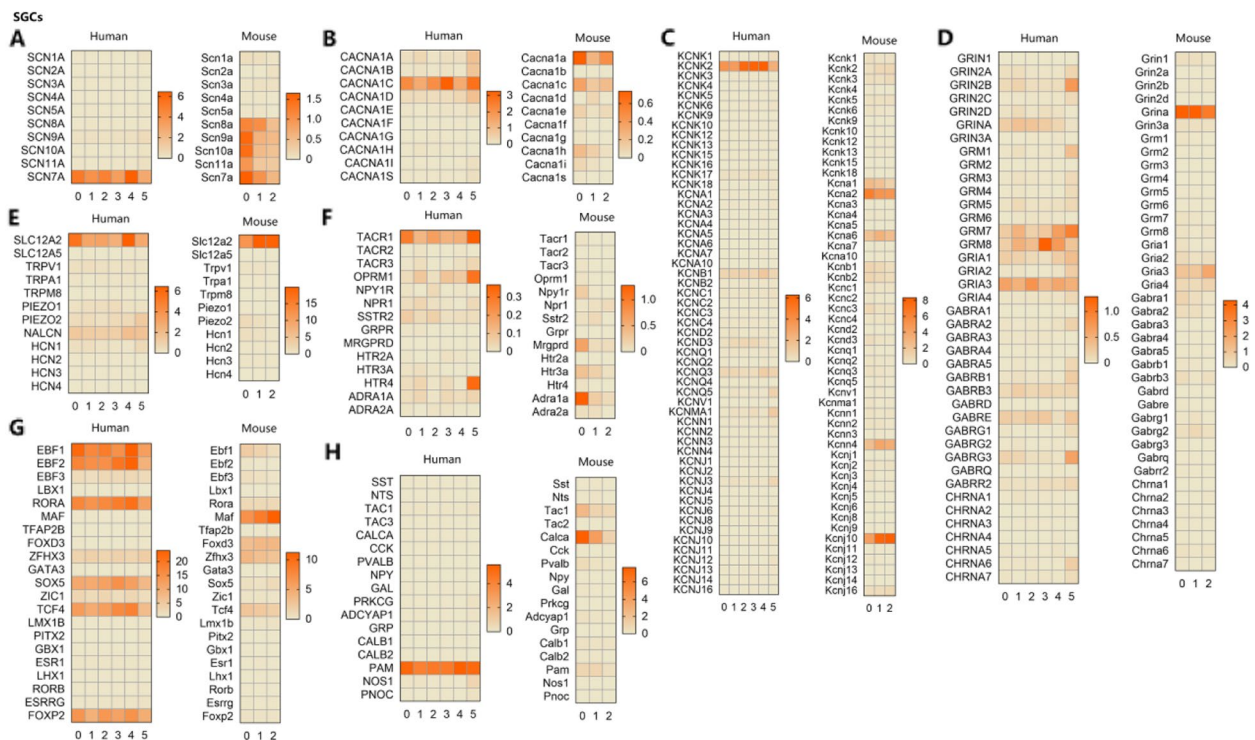


**Fig. 5** Expressional profiles of classical marker genes in DRG SGCs. Normalized mean gene expression of classic marker genes of sodium channels (A), calcium channels (B), potassium channels (C), glutamatergic-, GABAergic-, and cholinergic receptor (D), classical ion channels (E), classical receptors (F), transcription factors (G), and neuropeptides (H) in GABA and mouse SGCs. DRG, dorsal root ganglia; SGCs, satellite glial cells

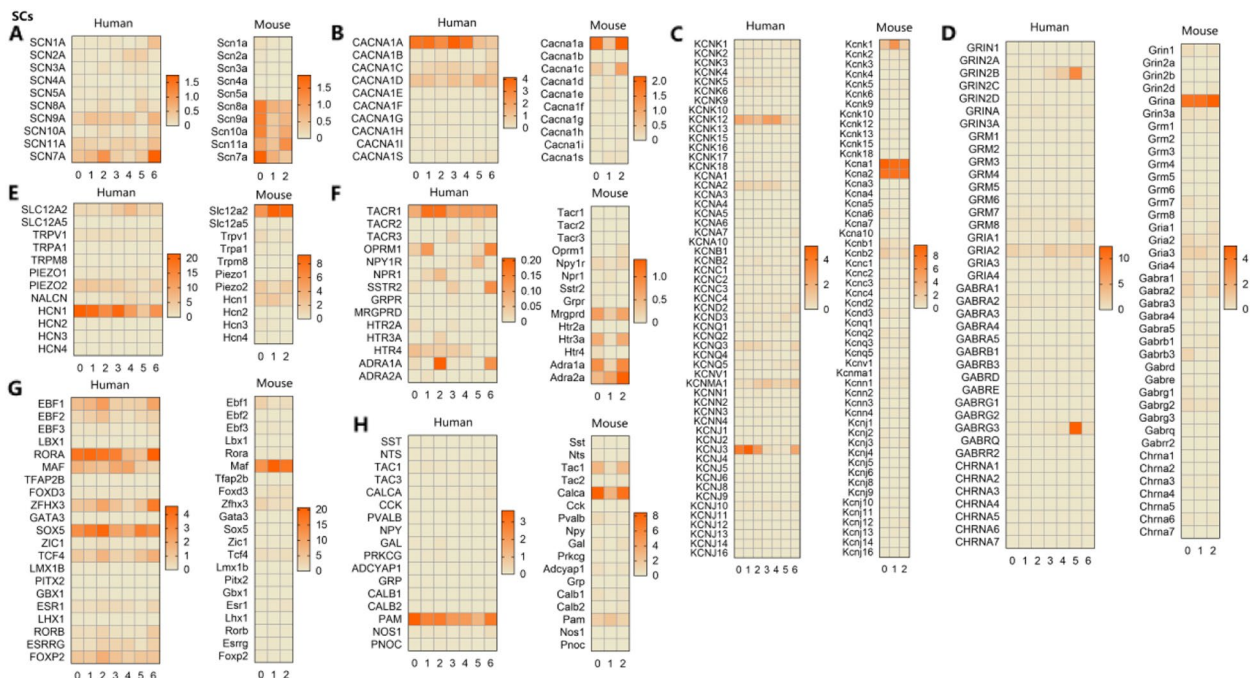


**Fig. 6** Expressional profiles of classical marker genes in DRG SCs. Normalized mean gene expression of classic marker genes of sodium channels (A), calcium channels (B), potassium channels (C), glutamatergic-, GABAergic-, and cholinergic receptor (D), classical ion channels (E), classical receptors (F), transcription factors (G), and neuropeptides (H) in human and mouse SCs. DRG, dorsal root ganglia; SCs, Schwann cells

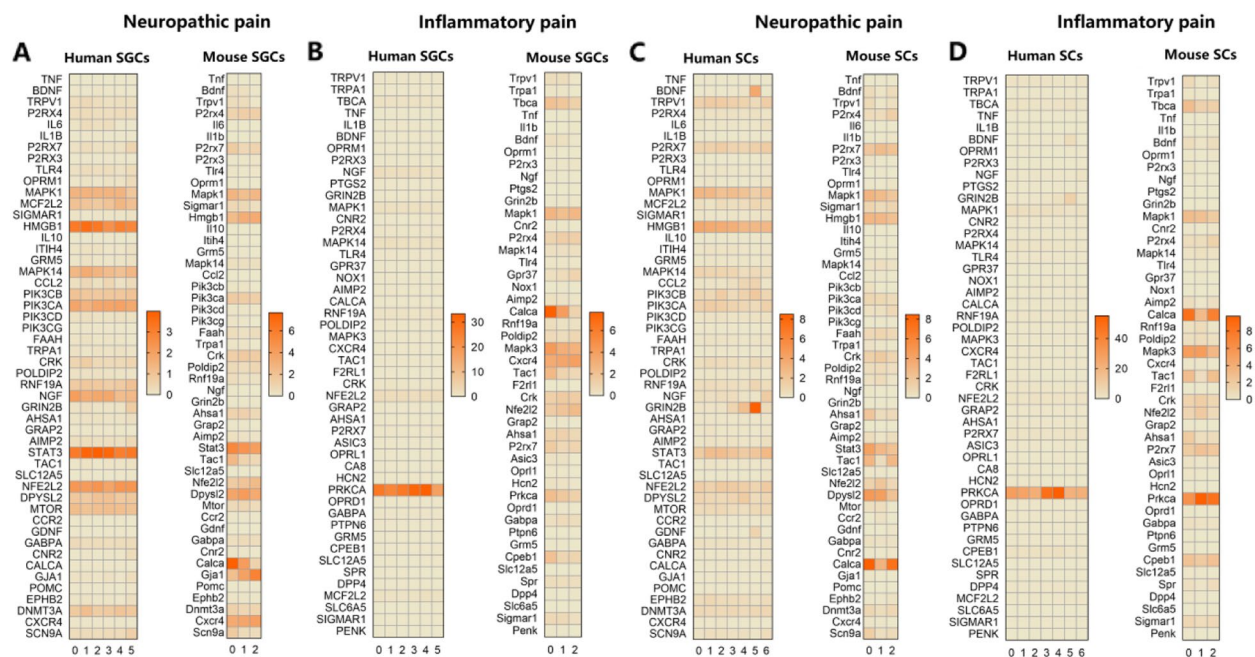


**Fig. 7** Expressional profiles of disease-risk genes in SGCs and SCs. **A, B** The transcriptional profiles of risk genes for neuropathic pain (**A**) and inflammatory pain (**B**) in human and mouse SGCs. **C, D** The transcriptional profiles of risk genes for neuropathic pain (**C**) and inflammatory pain (**D**) in human and mouse SCs. SGCs, satellite glial cells; SCs, Schwann cells

(Fig. 6F, left panel), but *Tacr1* expression was significantly lower than *Adra2a* in mouse SCs (Fig. 6F, right panel).

### 3.4 Disease-associated genes in glial cells

To better understand the conservation and divergence of genes associated with DRG-related diseases between humans and mice, we examined and compared the transcriptional profiles of these risk genes in two types of chronic pain, namely, neuropathic and inflammatory pain (Fig. 7). Several neuropathic pain-related genes, including *MAPK1/Mapk1* (encoding mitogen-activated protein kinase 1, which acts as an integration point for multiple biochemical signals), *HMGB1/Hmgb1* (encoding high mobility group box 1, which plays a role in inflammation process), and *STAT3/stat3* (encoding signal transducer and activator of transcription 3, which mediates the expression of various genes in response to cell stimuli) showed high expression levels in SGCs of both humans (Fig. 7A, left panel) and mice (Fig. 7A, right panel). Notably, *NGF* (encoding nerve growth factor, which is involved in the regulation of growth and differentiation of sympathetic and certain sensory neurons) showed higher expression than *CALCA*, *GJA1* (encoding gap junction protein alpha 1, which is associated with cell-cell gap junctions), and *CXCR4* (encoding C-X-C motif chemokine receptor 4, which is associated with pain signaling) in human SGCs (Fig. 7A, left panel), but *Ngf* was significantly lower than

*Calca*, *Gja1*, and *Cxcr4* in mouse SGCs (Fig. 7A, right panel). The inflammatory pain-related gene *PRKCA* (encoding protein kinase C alpha), which modulates different cellular processes, such as cell adhesion and cell transformation, showed extremely high expression levels than the other genes in human SGCs (Fig. 7B, left panel) and SCs (Fig. 7D, left panel). Several neuropathic pain-related genes, including *BDNF* (encoding brain derived neurotrophic factor, which is involved in many neurodegenerative disorders) and *GRIN2B* (encoding glutamate ionotropic receptor NMDA type subunit 2B, which acts as an agonist binding site for glutamate) were selectively highly expressed in Cluster 5 of human SCs (Fig. 7C, left panel).

### 3.5 Functional assignment for glial clusters

A Gene Ontology (GO) term analysis was performed to explore the functional properties of the enriched genes in glial cells and their subtypes; its results showed several common biological processes between humans and mice. The enriched genes in human SGCs were mainly associated with extracellular matrix organization, neuron migration, axon guidance, cell matrix adhesion, modulation of chemical synaptic transmission, and neuron projection development (Supplementary Fig. 5A). The enriched genes in human SCs were mainly associated with myelination, cell migration,



peripheral nervous system myelin maintenance, extracellular matrix organization, cell–cell adhesion, and regulation of dendritic spine development (Supplementary Fig. 6A). The enriched genes in mouse SGCs were mainly associated with myelination, regulation of oligodendrocyte differentiation, regulation of cell population proliferation, neuron projection development, extracellular matrix organization (Supplementary Fig. 7A). The enriched genes in mouse SCs were mainly associated with myelination, axon regeneration, transmission of nerve impulse, peripheral nervous system myelin formation and maintenance, and cell migration, regulation of cell population proliferation (Supplementary Fig. 7E). Detailed information on the GO term analysis for glial cell types and their subtypes were shown in Supplementary Figs. 5, 6, 7.

#### 4 Discussion

Despite the emerging evidence of the existence of distinct transcriptional profiles in glial cells from animal models [3, 6, 8, 9], little information is known about the heterogeneity within glial cells from human tissues at single-cell resolution. To the best of our knowledge, this is the first study to characterize the cellular and molecular complexity of glial cells, including SGCs and SCs in the human DRG using 10×Genomics snRNA-seq. Furthermore, we compared human transcriptomic data with those from mice to explore conservation and divergence across species. Additionally, we examined the expression profiles of genes associated with two types of chronic pain conditions in human DRG glial cells.

The biological function of SGCs has been less studied than that of their CNS counterparts, astrocytes. SGCs envelop neurons in the PNS, mainly including the sensory, parasympathetic, and sympathetic ganglia [24]. SGCs activity is altered after neuronal injury in peripheral sensory ganglia, such as the DRG and trigeminal ganglia [25–28]. Despite the clear evidence that SGCs play an important role in the PNS, little information is available regarding their cellular and molecular heterogeneity. Van Weperen et al. performed scRNA-seq of mouse stellate ganglia and identified six distinct subtypes based on transcriptomic profiles [3]. However, our findings showed that SGCs cannot be completely distinguished into different subtypes either in human or in mouse DRG, suggesting low cellular heterogeneity within DRG SGCs.

There is always an unsatisfying failure to translate preclinical mechanisms of peripheral pain and/or neurodegenerative disorders from rodents into clinical effective pain therapeutics [29–32]. A potential explanation is that important interspecies differences in molecular phenotypes exist between rodents and humans, as supported

by bulk RNA sequencing or RNAscope in situ hybridization [33–36]. Therefore, it is necessary to address the similarities and differences in gene expression profiles of peripheral nervous system between humans and mice, as most preclinical studies are conducted in mice. Recently, increasing studies have attempted to explore the similarities and differences between human and mouse DRG neurons at single-cell resolution. Nguyen et al. used single nuclear transcriptomics to characterize transcriptomic classes of human DRG neurons, which showed substantial similarity between human and mouse [14]. Tavares-Ferreira et al. used spatial transcriptomics to molecularly characterize transcriptomes of single human DRG neurons. They also compared human DRG neuronal subtypes to nonhuman primates and mice, and the results showed conserved patterns of gene expression among many cell types but divergence among specific nociceptor subsets [13]. Consistently, similar cell-type-specific gene expression patterns were observed between human and mouse TG neurons [12]. However, the information of divergence of glial cells between species was significantly less than that in neurons. Geirsdottir et al. reported that human microglia show significant heterogeneity in comparison with all mammals [5]. They further compared the expression of neurodegenerative disease susceptibility genes in human microglia with those of other mammalian species [5]. Their findings showed significant expression changes in susceptibility genes for Alzheimer's and Parkinson's disease in humans compared with in rodents. In the present study, our snRNA-seq data also suggested that SGCs and SCs exhibit substantial heterogeneity between humans and mice, as indicated by the slight overlap of their transcriptomic profiles. Furthermore, a number of genes showed differential expression patterns between mice and humans. Additionally, we compared the transcriptional data of human glial cells with those from mice in two common types of chronic pain, namely, neuropathic and inflammatory pain. As a result, some degree of heterogeneity in the expression levels of several genes was identified between humans and mice. For instance, previous study showed that *Cxcr4* were widely expressed in rodents DRG SGCs [37] and *CXCR4* signaling was associated with nerve injury-induced neuropathic pain [38]. In our study, *Cxcr4* was also highly expressed in mouse SGCs when compared to other genes (e.g., *Ngf*), however, it was little in humans when compared to other genes (e.g., *NGF*). In addition to *Cxcr4*, many disease-related genes were found highly expressed in mouse glial cells but little in humans, such as *Calca*, *Gja1*, and *Kcnj10*. Moreover, several classical genes associated with nociceptive signaling, such as *Scn10a*, *Maf*, and *Kcna2*, were also differentially expressed in DRG SGCs between

humans and mice. These heterogeneous gene expression patterns between humans and mice may partially explain the failure in the transition from animal models to clinical trials. Therefore, this work provides an important background to investigate the expression profiles of molecular targets of interest as well as their function in glial cells for DRG-related disease. A limitation is that the different platform used for mouse (inDrops) and human (10×Genomics) DRGs sequencing may influence the comparability between species.

This study has several limitations. First, the comparative results will be more rigorous if human and mouse samples in the same conditions. More importantly, the sequencing results from chronic pain patients will be of greater significance than those from patients without pain. Unfortunately, we have not obtained samples from these patients, and future studies may resolve this problem. Second, scRNA-seq will provide more integrated information than the snRNA-seq used in our study, and the molecular difference in the cytoplasm across species may also be associated with the failure of preclinical drug development. Therefore, it is interesting and meaningful to detect the molecular differences in the cytoplasm of DRG glial cells between human beings and rodents using scRNA-seq in future studies. Third, given that we only showed the expressional pattern of chronic pain-related genes in the peripheral glial cells, it is not clear about these genes in the central nervous system. The similarities and differences between the peripheral and central nervous system in the chronic pain-related genes may also help to develop therapeutic targets for sensation disorders.

In summary, our study provides a map of the complex cellular composition and transcriptomic atlas of glial cells in the human DRG. Our results also provide an essential resource of conserved and divergent expression profiles in glial cells between humans and mice. Importantly, this dataset not only offers the possibility to develop somatosensory disorders-related targets based on human transcriptomics, but also will serve as a valuable resource for translational researches on conserved molecular targets across species.

#### Abbreviations

DRG	Dorsal root ganglia
SGCs	Satellite glial cells
SCs	Schwann cells
GO	Gene Ontology
PNS	Peripheral nervous system
CNS	Central nervous system
scRNA-seq	Single-cell RNA sequencing
snRNA-seq	Single-nucleus RNA sequencing
BSA	Bovine serum albumin
PBS	Phosphate buffered saline
GEM	Gel beads in emulsion

UMI	Unique molecular identifier
HVGs	Highly variable genes
PCA	Principal component analysis
UMAP	Uniform Manifold Approximation and Projection
GDA	Gene-disease associations

## Supplementary Information

The online version contains supplementary material available at <https://doi.org/10.1007/s44254-023-00015-5>.

**Additional file 1: Supplementary figure 1.** (A) UMAP plot shows the contribution of each donor for cluster formation. Dots, individual cells; Colors, individual donor. (B) The ratio of each cluster in individual DRG. (C) The correlation analysis of gene expression among DRGs from three donors. Blue, positive correlation; Red, negative correlation; Smaller area of the ellipse means stronger correlation. UMAP, Uniform Manifold Approximation and Projection. **Supplementary figure 2.** (A–B) Heatmap showing the expression of the top ten most differentially expressed genes across all the subclusters of DRG SGCs in human (A) and mouse (B). SGCs, satellite glial cells. **Supplementary figure 3.** (A–B) Heatmap showing the expression of the top ten most differentially expressed genes across all the subclusters of DRG SCs in human (A) and mouse (B). SCs, Schwann cells. **Supplementary figure 4.** (A–B) UMAP plot showing the co-clustering of SGCs (A) and SCs (B) between human and mouse. Dots, individual cells; Colors, species. UMAP, Uniform Manifold Approximation and Projection; SGCs, satellite glial cells; SCs, Schwann cells. **Supplementary figure 5.** (A–G) Summarized GO terms for the enriched genes in SGCs (A) and each subtype (B–G) of human DRG. SGCs, satellite glial cells. **Supplementary figure 6.** (A–H) Summarized GO terms for the enriched genes in SCs (A) and each subtype (B–H) of human DRG. SCs, Schwann cells. **Supplementary figure 7.** (A–D) Summarized GO terms for the enriched genes in mouse SGCs (A) and each subtype (B–D). (E–H) Summarized GO terms for the enriched genes in mouse SCs (E) and each subtype (F–H). SGCs, satellite glial cells; SCs, Schwann cells.

#### Acknowledgements

Thanks to Yang Yang from Basebio for providing data analysis assistance.

#### Authors' contributions

Conceptualization: Donghang Zhang and Cheng Zhou; Data curation: Donghang Zhang and Yiyong Wei; Methodology and project administration: Donghang Zhang, Yiyong Wei, Yali Chen, Hongjun Chen, Jin Li, and Yaoxin Yang; Writing—original draft: Donghang Zhang; Writing—review & editing: Donghang Zhang and Cheng Zhou. All authors have read and approved the manuscript.

#### Funding

This work was supported by the National Key Research and Development Program of China (Project No. 2020YFC2008400 and 2020YFC2008402) (To Cheng Zhou); Grant No. 81974164 (To Cheng Zhou) from the National Natural Science Foundation of China; Grant No. 2021M692276 (To Donghang Zhang) from China Postdoctoral Science Foundation; Grant No. 2022NSFSC1399 (To Donghang Zhang) from the Natural Science Foundation of Sichuan Province; Grant No. 21PJ014 (To Donghang Zhang) from Health Commission of Sichuan Province; and Grant No. 20HXBH144 (To Donghang Zhang) from Post-Doctor Research Project, West China Hospital, Sichuan University.

#### Availability of data and materials

The datasets generated during and/or analysed during the current study are available from the corresponding author on reasonable request.

#### Declarations

##### Ethics approval and consent to participate

This study has been approved by the Ethical Committee of the Affiliated Hospital of Zunyi Medical University (Approval No. KLL-2020-273, May 19, 2021). Written informed consent was signed before patient enrollment. The study protocol was in consistent with the ethical and legal guidelines.



**Consent for publication**

All authors gave their consent for publication.

**Competing interests**

The authors have no relevant financial or non-financial interests to disclose.

**Author details**

<sup>1</sup>Department of Anesthesiology, West China Hospital, Sichuan University, Chengdu 610041, China. <sup>2</sup>Laboratory of Anesthesia and Critical Care Medicine, National-Local Joint Engineering Research Centre of Translational Medicine of Anesthesiology, West China Hospital, Sichuan University, Chengdu 610041, China. <sup>3</sup>Department of Anesthesiology, Affiliated Hospital of Zunyi Medical University, Zunyi 563003, China. <sup>4</sup>Department of Intensive Care Unit, Affiliated Hospital of Zunyi Medical University, Zunyi 563003, China. <sup>5</sup>Department of Orthopedic Surgery, Affiliated Hospital of Zunyi Medical University, Zunyi 563003, China.

Received: 2 February 2023 Revised: 12 March 2023 Accepted: 31 March 2023

Published online: 24 July 2023

**References**

- Tsuda M. Modulation of Pain and Itch by Spinal Glia. *Neurosci Bull*. 2018;34(1):178–85. <https://doi.org/10.1007/s12264-017-0129-y>.
- Ximerakis M, Lipnick SL, Innes BT, Simmons SK, Adiconis X, Dionne D, et al. Single-cell transcriptomic profiling of the aging mouse brain. *Nat Neurosci*. 2019;22(10):1696–708. <https://doi.org/10.1038/s41593-019-0491-3>.
- Van Weperen VYH, Littman RJ, Arneson DV, Contreras J, Yang X, Ajiola OA. Single-cell transcriptomic profiling of satellite glial cells in stellate ganglia reveals developmental and functional axial dynamics. *Glia*. 2021;69(5):1281–91. <https://doi.org/10.1002/glia.23965>.
- Tasdemir-Yilmaz OE, Druckenbrod NR, Olukoya OO, Dong W, Yung AR, Bastille I, et al. Diversity of developing peripheral glia revealed by single-cell RNA sequencing. *Dev Cell*. 2021;56(17):2516–35.e8. <https://doi.org/10.1016/j.devcel.2021.08.005>.
- Geirsdottir L, David E, Keren-Shaul H, Weiner A, Bohlen SC, Neuber J, et al. Cross-species single-cell analysis reveals divergence of the primate microglia program. *Cell*. 2020;181(3):746. <https://doi.org/10.1016/j.cell.2020.04.002>.
- Floriddia EM, Lourenço T, Zhang S, van Bruggen D, Hilscher MM, Kukanja P, et al. Distinct oligodendrocyte populations have spatial preference and different responses to spinal cord injury. *Nat Commun*. 2020;11(1):5860. <https://doi.org/10.1038/s41467-020-19453-x>.
- Diaz-Castro B, Bernstein AM, Coppola G, Sofroniew MV, Khakh BS. Molecular and functional properties of cortical astrocytes during peripherally induced neuroinflammation. *Cell Rep*. 2021;36(6):109508. <https://doi.org/10.1016/j.celrep.2021.109508>.
- Hasel P, Rose IVL, Sadick JS, Kim RD, Liddelow SA. Neuroinflammatory astrocyte subtypes in the mouse brain. *Nat Neurosci*. 2021;24(10):1475–87. <https://doi.org/10.1038/s41593-021-00905-6>.
- Zheng J, Ru W, Adolacion JR, Spurgat MS, Liu X, Yuan S, et al. Single-cell RNA-seq analysis reveals compartment-specific heterogeneity and plasticity of microglia. *iScience*. 2021;24(3):102186. <https://doi.org/10.1016/j.isci.2021.102186>.
- Sousa C, Golebiewska A, Poovathingal SK, Kaoma T, Pires-Afonso Y, Martina S, et al. Single-cell transcriptomics reveals distinct inflammation-induced microglia signatures. *EMBO Rep*. 2018;19(11):e46171. <https://doi.org/10.15252/embr.201846171>.
- Marques S, Zeisel A, Codeluppi S, van Bruggen D, Mendanha Falcão A, Xiao L, et al. Oligodendrocyte heterogeneity in the mouse juvenile and adult central nervous system. *Science*. 2016;352(6291):1326–9. <https://doi.org/10.1126/science.aaf6463>.
- Yang L, Xu M, Bhuiyan SA, Li J, Zhao J, Cohrs RJ, et al. Human and mouse trigeminal ganglia cell atlas implicates multiple cell types in migraine. *Neuron*. 2022;110(11):1806–1821.e8. <https://doi.org/10.1016/j.neuron.2022.03.003>.
- Tavares-Ferreira D, Shiers S, Ray PR, Wangzhou A, Jeevakumar V, Sankaranarayanan I, et al. Spatial transcriptomics of dorsal root ganglia identifies molecular signatures of human nociceptors. *Sci Transl Med*. 2022;14(632):eabj8186. <https://doi.org/10.1126/scitranslmed.abj8186>.
- Nguyen MQ, von Buchholtz LJ, Reker AN, Ryba NJ, Davidson S. Single-nucleus transcriptomic analysis of human dorsal root ganglion neurons. *Elife*. 2021;10:e71752. <https://doi.org/10.7554/eLife.71752>.
- Renthal W, Tochitsky I, Yang L, Cheng YC, Li E, Kawaguchi R, et al. Transcriptional reprogramming of distinct peripheral sensory neuron subtypes after axonal injury. *Neuron*. 2020;108(1):128–44.e9. <https://doi.org/10.1016/j.neuron.2020.07.026>.
- Gillespie CS, Sherman DL, Fleetwood-Walker SM, Cottrell DF, Tait S, Garry EM, et al. Peripheral demyelination and neuropathic pain behavior in periaxin-deficient mice. *Neuron*. 2000;26(2):523–31. [https://doi.org/10.1016/s0896-6273\(00\)81184-8](https://doi.org/10.1016/s0896-6273(00)81184-8).
- Zhu Y, Jones G, Tsutsui S, Opii W, Liu S, Silva C, et al. Lentivirus infection causes neuroinflammation and neuronal injury in dorsal root ganglia: pathogenic effects of STAT-1 and inducible nitric oxide synthase. *J Immunol*. 2005;175(2):1118–26. <https://doi.org/10.4049/jimmunol.175.2.1118>.
- Hu Z, Deng N, Liu K, Zhou N, Sun Y, Zeng W. CNTF-STAT3-IL-6 axis mediates neuroinflammatory cascade across schwann cell-neuron-microglia. *Cell Rep*. 2020;31(7):107657. <https://doi.org/10.1016/j.celrep.2020.107657>.
- Wang Q, Yang J, Wang H, Shan B, Yin C, Yu H, et al. Fibroblast growth factor 13 stabilizes microtubules to promote Na(+) channel function in nociceptive DRG neurons and modulates inflammatory pain. *J Adv Res*. 2021;31:97–111. <https://doi.org/10.1016/j.jare.2020.12.009>.
- Tavares-Ferreira D, Ray PR, Sankaranarayanan I, Mejia GL, Wangzhou A, Shiers S, et al. Sex differences in nociceptor translationalomes contribute to divergent prostaglandin signaling in male and female mice. *Biol Psychiatry*. 2022;91(1):129–40. <https://doi.org/10.1016/j.biopsych.2020.09.022>.
- Dawes JM, Weir GA, Middleton SJ, Patel R, Chisholm KI, Pettingill P, et al. Immune or genetic-mediated disruption of CASPR2 causes pain hypersensitivity due to enhanced primary afferent excitability. *Neuron*. 2018;97(4):806–22.e10. <https://doi.org/10.1016/j.neuron.2018.01.033>.
- Singhmar P, Trinh RTP, Ma J, Huo X, Peng B, Heijnen CJ, et al. The fibroblast-derived protein PL16 controls neuropathic pain. *Proc Natl Acad Sci U S A*. 2020;117(10):5463–71. <https://doi.org/10.1073/pnas.1913444117>.
- Stuart T, Butler A, Hoffman P, Hafemeister C, Papalexi E, Mauck WM, et al. Comprehensive integration of single-cell data. *Cell*. 2019;177(7):1888–902.e21. <https://doi.org/10.1016/j.cell.2019.05.031>.
- Hanani M. Satellite glial cells: more than just rings around the neuron. *Neuron Glia Biol*. 2010;6(1):1–2. <https://doi.org/10.1017/s1740925x10000104>.
- Shinder V, Govrin-Lippmann R, Cohen S, Belenky M, Ilin P, Fried K, et al. Structural basis of sympathetic-sensory coupling in rat and human dorsal root ganglia following peripheral nerve injury. *J Neurocytol*. 1999;28(9):743–61. <https://doi.org/10.1023/a:1007090105840>.
- Donegan M, Kernisant M, Cua C, Jasmin L, Ohara PT. Satellite glial cell proliferation in the trigeminal ganglia after chronic constriction injury of the infraorbital nerve. *Glia*. 2013;61(12):2000–8. <https://doi.org/10.1002/glia.22571>.
- Pannese E. The structure of the perineuronal sheath of satellite glial cells (SGCs) in sensory ganglia. *Neuron Glia Biol*. 2010;6(1):3–10. <https://doi.org/10.1017/s1740925x10000037>.
- Pannese E, Ledda M, Cherkas PS, Huang TY, Hanani M. Satellite cell reactions to axon injury of sensory ganglion neurons: increase in number of gap junctions and formation of bridges connecting previously separate perineuronal sheaths. *Anat Embryol (Berl)*. 2003;206(5):337–47. <https://doi.org/10.1007/s00429-002-0301-6>.
- Mogil JS. The translatability of pain across species. *Philos Trans R Soc Lond B Biol Sci*. 2019;374(1785):20190286. <https://doi.org/10.1098/rstb.2019.0286>.
- Renthal W, Chamesian A, Curatolo M, Davidson S, Burton M, Dib-Hajj S, et al. Human cells and networks of pain: transforming pain target identification and therapeutic development. *Neuron*. 2021;109(9):1426–9. <https://doi.org/10.1016/j.neuron.2021.04.005>.
- Sperling R, Mormino E, Johnson K. The evolution of preclinical Alzheimer's disease: implications for prevention trials. *Neuron*. 2014;84(3):608–22. <https://doi.org/10.1016/j.neuron.2014.10.038>.
- Yekkirala AS, Roberson DP, Bean BP, Woolf CJ. Breaking barriers to novel analgesic drug development. *Nat Rev Drug Discov*. 2017;16(8):545–64. <https://doi.org/10.1038/nrd.2017.87>.
- Ray P, Torck A, Quigley L, Wangzhou A, Neiman M, Rao C, et al. Comparative transcriptome profiling of the human and mouse dorsal root ganglia.

an RNA-seq-based resource for pain and sensory neuroscience research. *Pain*. 2018;159(7):1325–45. <https://doi.org/10.1097/j.pain.0000000000001217>.

34. Wangzhou A, McIvried LA, Paige C, Barragan-Iglesias P, Shiers S, Ahmad A, et al. Pharmacological target-focused transcriptomic analysis of native vs cultured human and mouse dorsal root ganglia. *Pain*. 2020;161(7):1497–517. <https://doi.org/10.1097/j.pain.0000000000001866>.
35. Middleton SJ, Barry AM, Comini M, Li Y, Ray PR, Shiers S, et al. Studying human nociceptors: from fundamentals to clinic. *Brain*. 2021;144(5):1312–35. <https://doi.org/10.1093/brain/awab048>.
36. Shiers S, Klein RM, Price TJ. Quantitative differences in neuronal subpopulations between mouse and human dorsal root ganglia demonstrated with RNAscope in situ hybridization. *Pain*. 2020;161(10):2410–24. <https://doi.org/10.1097/j.pain.0000000000001973>.
37. Bhangoo SK, Ren D, Miller RJ, Chan DM, Ripsch MS, Weiss C, et al. CXCR4 chemokine receptor signaling mediates pain hypersensitivity in association with antiretroviral toxic neuropathy. *Brain Behav Immun*. 2007;21(5):581–91. <https://doi.org/10.1016/j.bbi.2006.12.003>.
38. Dubový P, Klusáková I, Svizenská I, Brázda V. Spatio-temporal changes of SDF1 and its CXCR4 receptor in the dorsal root ganglia following unilateral sciatic nerve injury as a model of neuropathic pain. *Histochem Cell Biol*. 2010;133(3):323–37. <https://doi.org/10.1007/s00418-010-0675-0>.

### Publisher's Note

Springer Nature remains neutral with regard to jurisdictional claims in published maps and institutional affiliations.